Article

Cell Reports

ER Stress Protein CHOP Mediates Insulin Resistance by Modulating Adipose Tissue Macrophage Polarity

Graphical Abstract

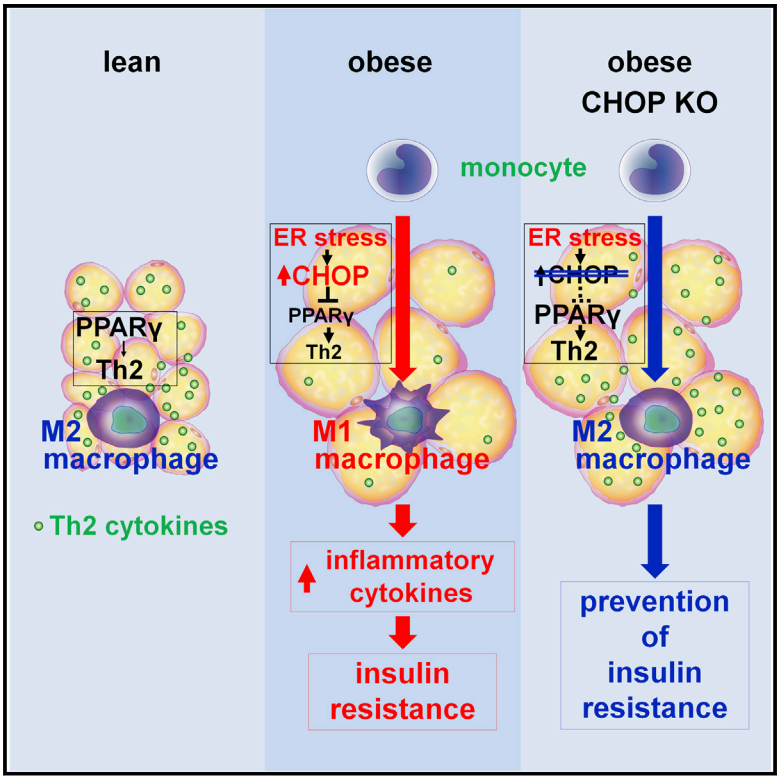

Authors

Toru Suzuki, Junhong Gao, Yasushi Ishigaki, ..., Tetsuya Yamada, Seiichi Oyadomari, Hideki Katagiri

Correspondence

katagiri@med.tohoku.ac.jp

In Brief

Suzuki et al. report that CHOP deficiency maintains ATM M2 polarization, thereby preventing insulin resistance during obesity development. CHOP upregulation in adipocytes alters micro-environmental conditions in WAT, involving suppression of Th2 cytokine production, resulting in ATM M1 polarization. This molecular mechanism may link adipose ER stress with systemic insulin resistance.

Highlights

- A high-fat diet (HFD) upregulates ER stress-related protein, CHOP, in adipocytes
- CHOP deficiency prevents HFD-induced insulin resistance with ATM M2 polarization
- M2 polarization involves more eosinophils and Th2 cytokines in WAT of CHOP$^{-/-}$ mice
- BMT experiments show recipient CHOP to be the major determinant of ATM polarity

Suzuki et al., 2017, Cell Reports *18*, 2045–2057
February 21, 2017
http://dx.doi.org/10.1016/j.celrep.2017.01.076

Cell Reports
Article

ER Stress Protein CHOP Mediates Insulin Resistance by Modulating Adipose Tissue Macrophage Polarity

Toru Suzuki,[1,7] Junhong Gao,[1,2,7] Yasushi Ishigaki,[3] Keiichi Kondo,[1] Shojiro Sawada,[1] Tomohito Izumi,[1] Kenji Uno,[1] Keizo Kaneko,[1] Sohei Tsukita,[1] Kei Takahashi,[1] Atsuko Asao,[4] Naoto Ishii,[4] Junta Imai,[1] Tetsuya Yamada,[1] Seiichi Oyadomari,[5] and Hideki Katagiri[1,6,8,*]

[1]Department of Metabolism and Diabetes, Tohoku University Graduate School of Medicine, 2-1 Seiryo-machi, Aoba-ku, Sendai, Miyagi 980-8575, Japan

[2]Tohoku University International Advanced Research and Education Organization, Frontier Research Institute for Interdisciplinary Science, 6-3 Aoba, Aramaki, Aoba-ku, Sendai, Miyagi 980-8578, Japan

[3]Division of Diabetes and Metabolism, Iwate Medical University, 19-1 Uchimaru, Morioka, Iwate 020-8505, Japan

[4]Department of Microbiology and Immunology, Tohoku University Graduate School of Medicine, 2-1 Seiryo-machi, Aoba-ku, Sendai, Miyagi 980-8575, Japan

[5]Division of Molecular Biology, Institute for Genome Research, University of Tokushima, 3-18-15 Kuramoto, Tokushima 770-8503, Japan

[6]Agency for Medical Research and Development-Core Research for Evolutional Medical Science and Technology (AMED-CREST), Japan Agency for Medical Research and Development, Chiyoda-ku, Tokyo 100-1004, Japan

[7]Co-first author

[8]Lead Contact

*Correspondence: katagiri@med.tohoku.ac.jp

http://dx.doi.org/10.1016/j.celrep.2017.01.076

SUMMARY

Obesity represents chronic inflammatory states promoted by pro-inflammatory M1-macrophage infiltration into white adipose tissue (WAT), thereby inducing insulin resistance. Herein, we demonstrate the importance of an ER stress protein, CHOP, in determining adipose tissue macrophage (ATM) polarity and systemic insulin sensitivity. A high-fat diet (HFD) enhances ER stress with CHOP upregulation in adipocytes. CHOP deficiency prevents HFD-induced insulin resistance and glucose intolerance with ATM M2 predomination and Th2 cytokine upregulation in WAT. Whereas ER stress suppresses Th2 cytokine expression in cultured adipocytes, CHOP knockdown inhibits this downregulation. In contrast, macrophage responsiveness to Th1/Th2 cytokines is unchanged regardless of whether CHOP is expressed. Furthermore, bone marrow transplantation experiments showed recipient CHOP to be the major determinant of ATM polarity. Thus, CHOP in adipocytes plays important roles in ATM M1 polarization by altering WAT micro-environmental conditions, including Th2 cytokine downregulation. This molecular mechanism may link adipose ER stress with systemic insulin resistance.

INTRODUCTION

The endoplasmic reticulum (ER) is an organelle that has essential roles in multiple cellular processes required for normal cellular functions and cell survival. When ER homeostasis is disrupted, unfolded proteins accumulate in the ER lumen, subsequently activating unfolded protein responses (UPRs), also known as ER stress responses (Ron and Walter, 2007). Various disturbances, including ischemia, hypoxia, oxidative injury, and viral infections, trigger protein unfolding in the ER and lead to UPRs (Ron and Walter, 2007). Recent studies have revealed that ER stress is associated with a wide range of diseases, including neurodegenerative disorders (Niwa et al., 1999), cancer (Bi et al., 2005), atherosclerosis (Gao et al., 2011), and deterioration of pancreatic β-cells (Ishihara et al., 2004; Oyadomari et al., 2002; Wang et al., 1999). The UPR is an adaptive response that first tends to restore ER activity and cellular homeostasis but shifts toward apoptosis when ER stress is severe and/or prolonged. The transcription factor C/EBP homologous protein (CHOP) is a downstream component of ER stress pathways and is well known to mediate cellular apoptosis (Oyadomari and Mori, 2004). In particular, CHOP deficiency suppresses β-cell loss in murine models of ER stress-mediated diabetes (Oyadomari et al., 2002) and type 2 diabetes (Song et al., 2008).

In addition to pancreatic β-cell apoptosis, ER stress is considered to play crucial roles in the development of insulin resistance associated with obesity (Nakatani et al., 2005). Although female CHOP$^{-/-}$ mice reportedly gain weights with increased adiposity and hepatic steatosis (Ariyama et al., 2007; Maris et al., 2012), these mice maintain normal glucose tolerance associated with lower levels of pro-inflammatory cytokines (Maris et al., 2012). We also reported that CHOP deficiency inhibits both types of arteriosclerosis in the processes of cuff injury-induced neointimal formation and hypercholesterolemia-induced atherosclerosis, with suppressed aortic expressions of inflammatory factors (Gao et al., 2011). Thus, CHOP has a role in mediating pro-inflammatory responses

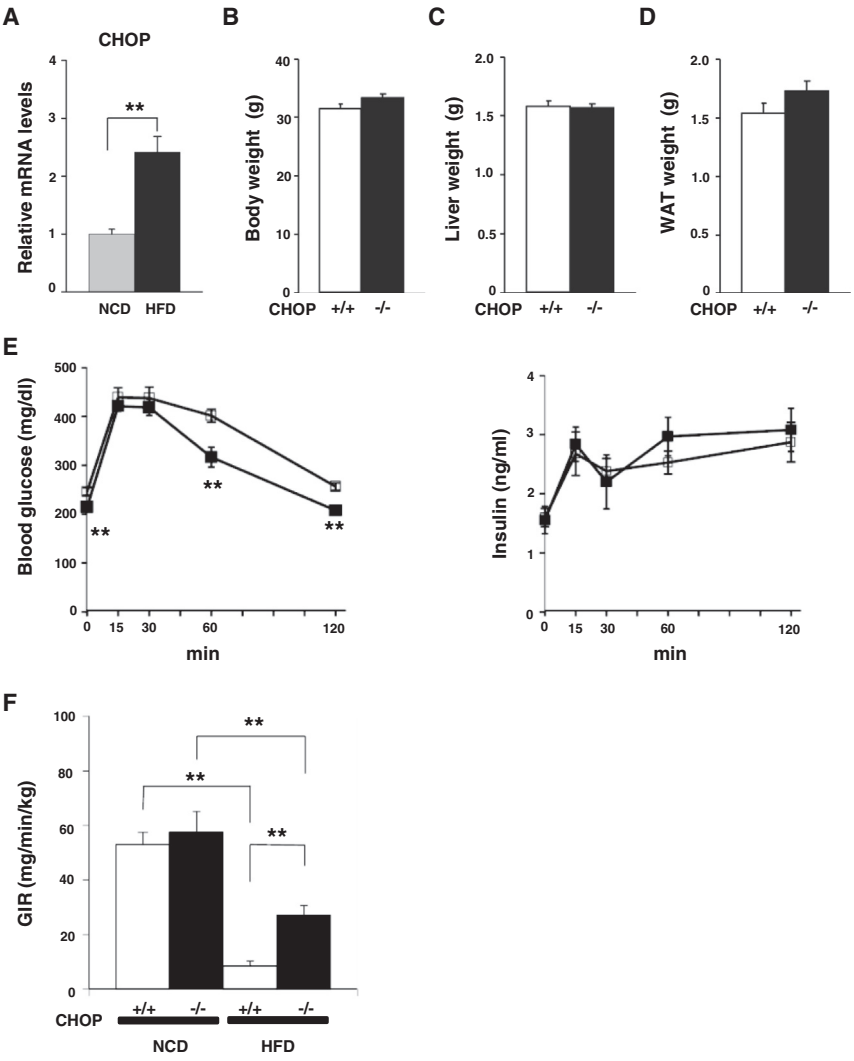

Figure 1. CHOP Deficiency Prevents Insulin Resistance under HFD-Feeding Conditions

$CHOP^{+/+}$ (white bars) and $CHOP^{-/-}$ (black bars) mice were fed the HFD for 6 weeks beginning at the age of 6 weeks and underwent comparative analyses with mice of the same age, having these genotypes and being fed the NCD at the same age.

(A) Relative amounts of mRNA for CHOP in the adipocyte fractions obtained from WAT of NCD-fed (gray bar) and HFD-fed (white bar) $CHOP^{+/+}$ mice were measured (n = 6–10 per group).

(B–D) Body (B), liver (C), and WAT (D) weights were measured in HFD-fed $CHOP^{+/+}$ and $CHOP^{-/-}$ mice (n = 20–22 per group).

(E) Blood glucose (left panel) and plasma insulin (right panel) levels in HFD-fed $CHOP^{+/+}$ (open square, n = 6–8) and $CHOP^{-/-}$ (closed square, n = 8) mice were measured during intraperitoneal glucose tolerance tests.

(F) Glucose infusion rates (GIRs) during hyperinsulinemic-euglycemic clamp procedures were measured in NCD-fed and HFD-fed $CHOP^{+/+}$ and $CHOP^{-/-}$ mice (n = 6–8 per group). Data are presented as means ± SEM. *p < 0.05, **p < 0.01 by one-way ANOVA.

in addition to its well-known apoptotic role (Gao et al., 2011). These findings, taken together, prompted us to postulate that, in adipose tissue as well, CHOP plays important roles in pro-inflammatory responses, thereby contributing to the development of insulin resistance.

Obesity is considered to be a chronic inflammatory state that is augmented by macrophage infiltration into white adipose tissue (WAT) (Wellen and Hotamisligil, 2003; Xu et al., 2003). Recent evidence has suggested that adipose tissue macrophages (ATMs) have a variety of characteristics. In particular, classically activated (M1) macrophages produce excessive quantities of pro-inflammatory cytokines, whereas alternatively activated (M2) macrophages are characterized by attenuating excessive inflammation (Gordon, 2003; Gordon and Taylor, 2005; Mantovani et al., 2004). Whereas M2 macrophages are predominant in adipose tissue in lean states (Feuerer et al., 2009), high-fat diet (HFD) feeding is well known to trigger the recruitment of M1 macrophages, which is an important cause of insulin resistance (Lumeng et al., 2007). Interestingly, in the present study, we found that, in $CHOP^{-/-}$ mice, HFD feeding caused infiltration of similar amounts of macrophages into WAT, the phenotype of which was predominantly M2, leading to the prevention of insulin resistance. Bone marrow transplantation (BMT) experiments revealed ATM polarization to be dependent on the presence of recipient CHOP, suggesting that CHOP-mediated, i.e., ER stress-induced, micro-environmental alterations within WAT play essential roles in the induction of M1 polarization of infiltrating macrophages during obesity development, which in turn leads to systemic insulin resistance.

RESULTS

CHOP Deficiency Inhibited HFD-Induced Glucose Intolerance by Preventing Insulin Resistance

To examine the effects of CHOP deficiency on glucose metabolism and insulin sensitivity in the state of HFD-induced obesity, $CHOP^{+/+}$ and $CHOP^{-/-}$ mice were fed a 32% fat chow for 6 weeks starting at the age of 6 weeks and underwent comparative analyses of mice, the same age, with these genotypes fed a normal chow diet (NCD). At the end of this HFD feeding period, in $CHOP^{+/+}$ mice, CHOP expression was significantly upregulated in WAT at both mRNA and protein levels (Figures S1A and S1B). When WAT was separated into the floating adipocyte and the stromal vascular (SV) fractions, CHOP upregulation was remarkable in the adipocyte fractions (Figure 1A). As was the case with CHOP, other ER stress-related proteins, such as Bip, ATF4, and ATF6, were also upregulated in

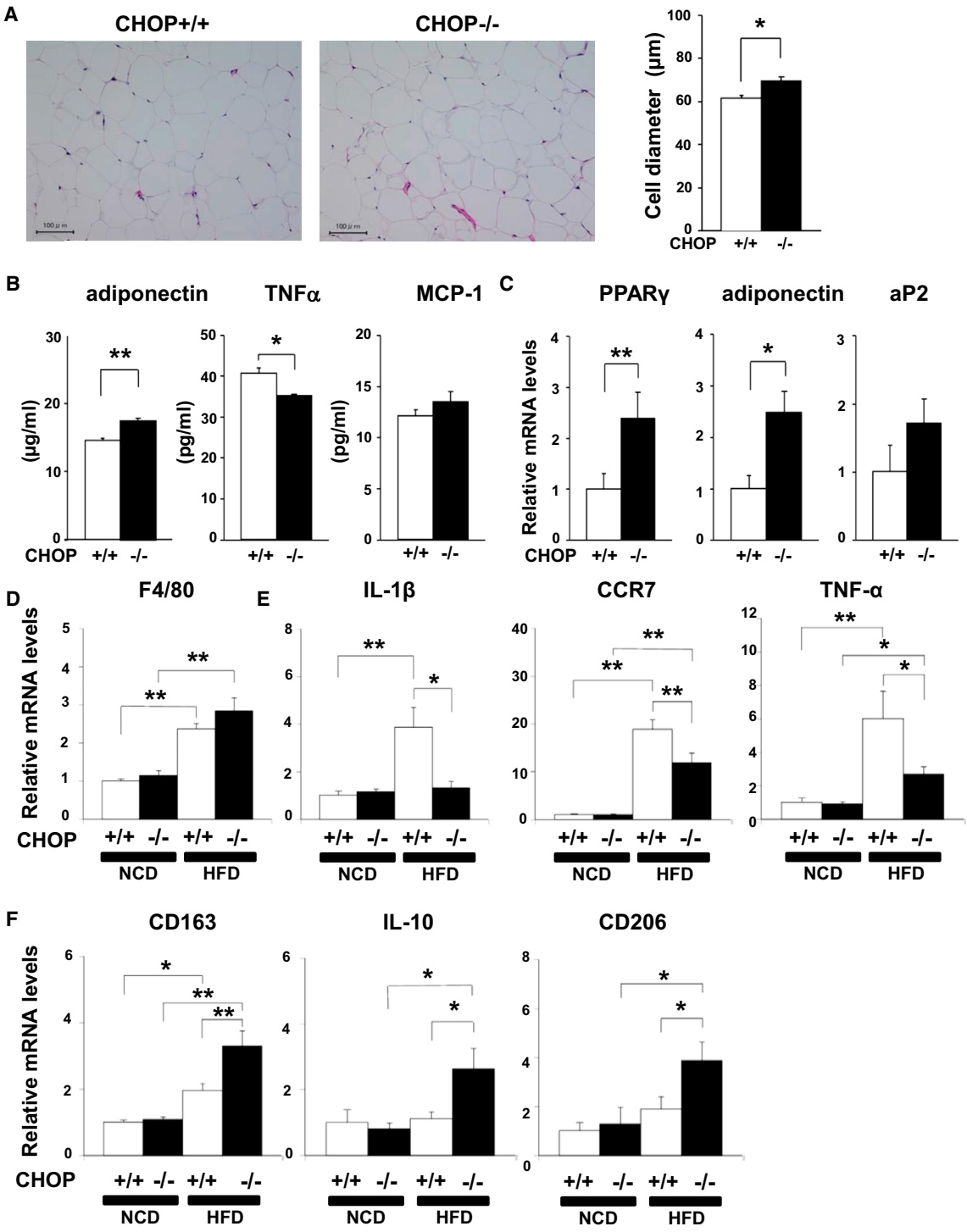

Figure 2. CHOP Deficiency Induces ATM Polarization to the M2 Phenotype

$CHOP^{+/+}$ (white bars) and $CHOP^{-/-}$ (black bars) mice were fed the HFD for 6 weeks.

(A) WAT sections (H&E staining) were histologically analyzed, and adipocyte diameters were measured in HFD-fed $CHOP^{+/+}$ and $CHOP^{-/-}$ mice (n = 19–21 per group). Cell diameters of at least 100 adipocytes per mouse in each group were traced manually and analyzed (right panel).

(B) Plasma adipokines, such as adiponectin (left), TNF-α (middle), and MCP-1 (right), were measured in HFD-fed $CHOP^{+/+}$ (n = 10) and $CHOP^{-/-}$ (n = 11–13) mice.

(legend continued on next page)

WAT by HFD feeding, and the upregulations of these ER stress-related proteins were similarly observed in CHOP$^{-/-}$ mice (Figure S1C). In addition, expressions of apoptosis-related proteins, such as Bcl2 (Nagel et al., 2014) and CD95 (Rapold et al., 2013), did not differ between WAT from CHOP$^{+/+}$ and CHOP$^{-/-}$ mice (Figure S2A). Consistent with a previous report (Strissel et al., 2007), TUNEL staining of WAT revealed that HFD loading for 6 weeks did not increase TUNEL-positive cells in WAT of either CHOP$^{+/+}$ or CHOP$^{-/-}$ mice (Figures S2B and S2C). In addition, no significant differences in the ratios of TUNEL-positive to total nuclei were observed between CHOP$^{+/+}$ and CHOP$^{-/-}$ mice. These findings suggest that HFD loading for 6 weeks substantially increased ER stress in WAT, irrespective of CHOP expression, whereas it is unlikely that CHOP-mediated apoptosis had yet occurred in WAT at this time point.

First, under the NCD condition, CHOP deficiency exerted only minor impacts on overall body weight (Figure S3A), fasting blood glucose (Figure S3B), and insulin (Figure S3C) levels, nor were plasma lipid parameters such as total cholesterol, triglycerides, and non-esterified fatty acids (NEFAs) (Figure S3D) significantly altered at 12 weeks of age. Furthermore, glucose tolerance tests revealed no significant differences in blood glucose levels either before or after glucose loading between these two genotypes (Figure S3E). Thus, under the NCD condition, CHOP deficiency exerted minimal effects on glucose metabolism and insulin sensitivity.

After loading of HFD for 6 weeks as well, body weights were similar in CHOP$^{+/+}$ and CHOP$^{-/-}$ mice (Figure 1B). It merits emphasis that liver weights (Figure 1C) and hepatic triglyceride contents (Figure S4A) did not differ between these two groups of mice. Furthermore, pancreatic insulin contents were similar between CHOP$^{+/+}$ and CHOP$^{-/-}$ mice (Figure S4B). Therefore, we selected this time point for HFD loading to focus on the role of CHOP in insulin resistance associated with HFD-induced obesity, as the influences of hepatic steatosis and pancreatic β-cell loss would be minimal.

WAT weights tended to be greater in CHOP$^{-/-}$ mice, although the difference did not reach statistical significance (Figure 1D). The food intake amounts (Figure S4C), locomotor activity (Figure S4D), and resting oxygen consumption during both the dark and the light phase (Figure S4E) did not differ between CHOP$^{+/+}$ and CHOP$^{-/-}$ mice. Fasting blood glucose levels were slightly but significantly lower in CHOP$^{-/-}$ than in CHOP$^{+/+}$ mice (Figure S4F), whereas fasting serum insulin levels (Figure S4G) and lipid parameters (Figure S4H) did not differ between the two groups. Glucose tolerance tests revealed that glucose elevation after a glucose load was also significantly suppressed in CHOP$^{-/-}$ mice with similar insulin secretion (Figure 1E), indicating preventive effects of CHOP deficiency on HFD-induced glucose intolerance.

In addition, we precisely analyzed insulin sensitivity employing the hyperinsulinemic-euglycemic clamp procedure (Figure 1F). Under the NCD condition, glucose infusion rates (GIRs) were similar in CHOP$^{+/+}$ and CHOP$^{-/-}$ mice. In CHOP$^{+/+}$ mice, HFD remarkably suppressed GIRs, by 84%, indicating the development of severe insulin resistance. In contrast, this decline in GIRs was significantly attenuated in CHOP$^{-/-}$ mice, i.e., the GIRs were 3.2-fold higher, than in CHOP$^{+/+}$ under the HFD condition (Figure 1F), indicating prevention of systemic insulin resistance. Collectively, these findings demonstrate CHOP deficiency to have markedly inhibited the development of HFD-induced glucose intolerance due mainly to prevention of insulin resistance.

CHOP Deficiency Induced ATM Polarization to Alternatively Activated M2-Macrophage Phenotype

Histological analyses of WAT showed that HFD markedly enlarged adipocytes in CHOP$^{+/+}$ mice and that CHOP deficiency further increased the diameters of adipocytes (Figure 2A). Despite apparent adipocyte hypertrophy, plasma adiponectin and tumor necrosis factor α (TNF-α) levels were significantly higher and lower, respectively, in CHOP$^{-/-}$ than in CHOP$^{+/+}$ HFD-fed mice, whereas monocyte chemoattractant protein-1 (MCP-1) levels were similar between these mice (Figure 2B). Furthermore, qRT-PCR revealed mRNA expressions of peroxisome proliferator-activated receptor-γ (PPARγ) and adiponectin to be significantly increased in WAT of CHOP$^{-/-}$ mice (Figure 2C), suggesting that adipocytes were normally differentiated and functioning well in CHOP$^{-/-}$ mice even when fed the HFD.

In addition, HFD increased the expressions of a macrophage marker F4/80 (Figure 2D) and MCP-1, which is involved in monocyte recruitment (Figure S5), in WAT of both CHOP$^{+/+}$ and CHOP$^{-/-}$ mice. These increases in WAT did not differ significantly between the two genotypes (Figures 2D and S5), indicating similar degrees of WAT macrophage infiltration in CHOP$^{+/+}$ and CHOP$^{-/-}$ mice. In contrast, although the markers of M1 macrophages, such as interleukin-1β (IL-1β), CCR7, and TNF-α, were dramatically increased by HFD in CHOP$^{+/+}$ mice, expressions of these M1 markers were significantly suppressed by CHOP deficiency (Figure 2E). In addition, intriguingly, the expressions of M2-macrophage markers, such as CD163, IL-10, and CD206, in WAT were markedly increased in CHOP$^{-/-}$ mice fed the HFD (Figure 2F). These findings suggest that M2 macrophages predominated in WAT of CHOP$^{-/-}$ mice.

We further confirmed M2 macrophages to be predominant in WAT of CHOP$^{-/-}$ mice employing immunohistochemistry and flow-cytometric procedures. First, immunostaining of WAT with antibodies against CD11c and CD206, cell surface markers for M1 and M2 macrophages, respectively, revealed that CD11c^{+} cells were decreased, whereas CD206^{+} cells were increased, in peri-adipocyte regions of WAT from CHOP$^{-/-}$ mice (Figure 3A). Next, we performed flow-cytometric analyses

(C) Relative amounts of mRNA for adipocyte differentiation-related proteins, such as PPARγ (left), adiponectin (middle), and aP2 (right) were determined in WAT of HFD-fed CHOP$^{+/+}$ and CHOP$^{-/-}$ mice (n = 11–13 per group) by qRT-PCR.

(D–F) Relative amounts of mRNA for macrophage markers, with F4/80 representing the entire macrophage population (D), M1 markers (E), and M2 markers (F), were determined in WAT of CHOP$^{+/+}$ and CHOP$^{-/-}$ mice fed an NCD (n = 6–7 per group) and HFD (n = 13 per group) by qRT-PCR. Data are presented as means ± SEM. *$p < 0.05$, **$p < 0.01$ by one-way ANOVA.

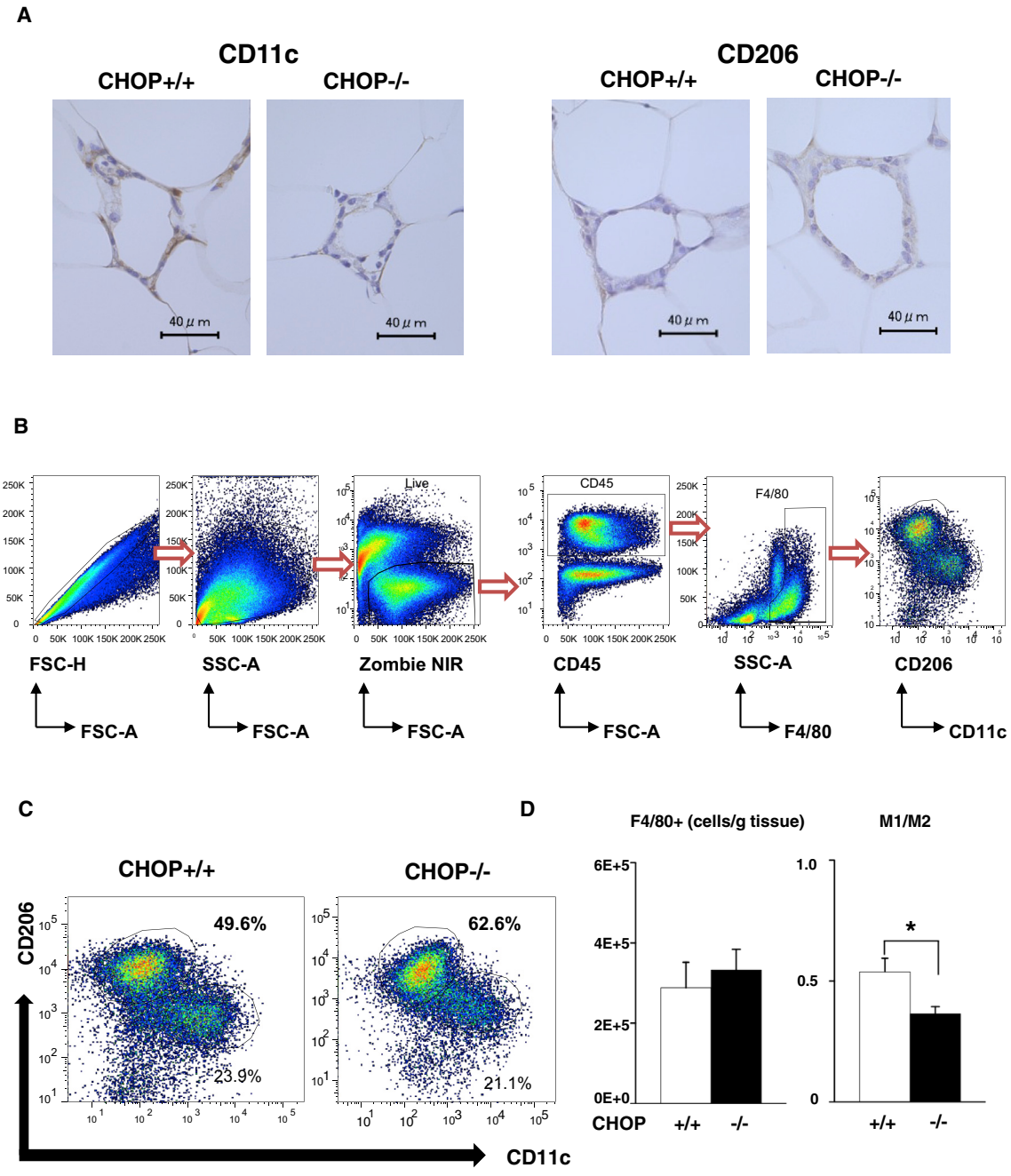

Figure 3. CHOP Deficiency Upregulates Th2 Cytokines in WAT, Leading to ATM Polarization to the M2 Phenotype

$CHOP^{+/+}$ (white bars) and $CHOP^{-/-}$ (black bars) mice were fed the HFD for 6 weeks.

(A) Epididymal adipose tissue was stained with anti-CD11c (left panels) or anti-CD206 (right panels) antibodies. Representative images are shown.

(B) Representative flow-cytometric plots of SVF cells isolated from epididymal adipose tissue. The dot plots depict forward scatter (FSC) and side scatter (SSC) and the sequential gating strategy for analysis of ATM.

(C) Presence of $CD45^+$ $F4/80^+$ cells and expressions of the macrophage markers, CD206 and CD11c, on ATMs. The sequential gating for $F4/80^+$ macrophages, as well as the M1-like $CD11c^+$ and $CD206^+$ macrophages, is shown. The abundances of all macrophages as well as those with the M1 and M2 phenotypes were calculated.

(D) The total number of $F4/80^+$ cells (left panel) and the ratio of M1/M2 macrophages (right panel) (n = 5 per group). Data are presented as means ± SEM. *$p < 0.05$ by the unpaired t test.

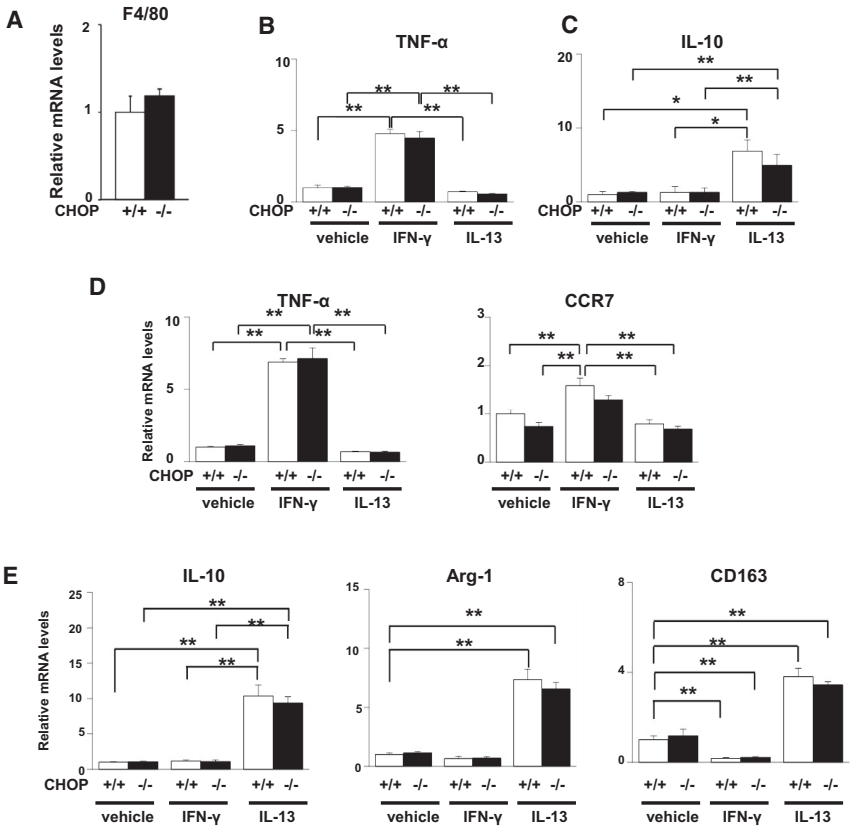

Figure 4. CHOP Deficiency in Macrophages Does Not Affect M1/M2 Transition in Response to Cytokine Stimulations

(A) Relative amounts of mRNA expressions for F4/80 was determined in the peripheral blood of CHOP$^{+/+}$ (white bars) and CHOP$^{-/-}$ (black bars) mice fed HFD.

(B–E) Monocytes/macrophages were collected from the spleens of CHOP$^{+/+}$ (white bars) and CHOP$^{-/-}$ (black bars) mice by magnetic cell sorting (B and C). Bone marrow-derived macrophages were harvested from the bone marrow cells of CHOP$^{+/+}$ (white bars) and CHOP$^{-/-}$ (black bars) mouse femurs (D and E). Splenic monocytes/macrophages (B and C) and bone marrow-derived macrophages (D and E) were incubated with or without 20 ng/mL recombinant IFN-γ or 10 ng/mL recombinant IL-13 for 24 hr. Relative amounts of mRNA expressions for makers of M1 (B and D) and M2 (C and E) macrophages were determined by qRT-PCR (n = 7–8 per group). Data are presented as means ± SEM. *p < 0.05, **p < 0.01 by one-way ANOVA.

of the SV fractions of WAT (Figure 3B). Although total macrophages (F4/80^{+}) were similar for both genotypes, the ratio of M1 (F4/80^{+}CD11c^{+}CD206^{-})/M2 (F4/80^{+}CD11c^{-}CD206^{+}) macrophages was significantly lower in CHOP$^{-/-}$ mice (Figure 3C). Taken together, these observations indicate that, despite similar amounts of macrophage infiltration in WAT, CHOP deficiency increased M2 polarization of ATMs, thereby attenuating HFD-induced insulin resistance.

Th2 Cytokine Upregulation in Adipocytes Due to CHOP Deficiency Promoted ATM Polarization to the M2 Phenotype

What mechanism underlies the ATM polarization to the M2 phenotype in WAT of CHOP$^{-/-}$ mice? We next examined whether CHOP expressed in macrophages affects M1/M2 polarization. First, F4/80 expressions in peripheral blood were similar in CHOP$^{+/+}$ and CHOP$^{-/-}$ mice (Figure 4A). Next, we examined whether CHOP-deficient monocytes/macrophages per se are prone to undergo the M2, rather than the M1, transition. It is well known that rich Th2 (mainly IL-13) circumstances in adipose tissue maintain ATM M2 predomination in lean mice, whereas, under obesity conditions, Th1 (e.g., interferon-γ [IFN-γ]) (Sica and Mantovani, 2012) and Th2 (e.g., IL-13) (Kang et al., 2008) cytokines increase and decrease, respectively, leading to the M1 phenotype becoming predominant (Goerdt et al., 1999; Gordon, 2003). Therefore, we analyzed the responsiveness of macrophages to IFN-γ and IL-13 ex vivo. First, we collected monocytes/macrophages from the spleens of CHOP$^{+/+}$ and CHOP$^{-/-}$ mice using the magnetic cell-sorting procedure. Treatment with IFN-γ and IL-13 similarly upregulated TNF-α and IL-10, respectively, in splenic monocytes/macrophages obtained from CHOP$^{+/+}$ and CHOP$^{-/-}$ mice (Figures 4B and 4C). In addition, we further examined the responsiveness of macrophages derived from bone marrow of CHOP$^{+/+}$ and CHOP$^{-/-}$ mice, to IFN-γ and IL-13, because the majority of macrophages infiltrating adipose tissue during high-fat feeding are reportedly bone marrow derived (Boutens and Stienstra, 2016; Koh et al., 2007). Consistently, treatment with IFN-γ similarly upregulated M1 markers, such as TNF-α and CCR7, in bone marrow-derived macrophages obtained from CHOP$^{+/+}$ and CHOP$^{-/-}$ mice (Figure 4D). In addition, treatment with IL-13 upregulated M2 markers, such as IL-10, Arg-1, and CD163, in both CHOP$^{+/+}$ and CHOP$^{-/-}$ macrophages, and the upregulations were not statistically different (Figure 4E). Taken together with the results obtained from our ex vivo experiments, it is unlikely that CHOP deficiency in macrophages is responsible for the ATM M2 polarization observed in CHOP$^{-/-}$ mice.

Therefore, we next focused on micro-environmental conditions in the vicinity of macrophages that had infiltrated and remained within WAT. Th2 cytokines, such as IL-4 and IL-13, reportedly play major roles in macrophage polarization to the M2 phenotype in WAT (Van Dyken and Locksley, 2013). Consistent with this notion, HFD feeding markedly suppressed these Th2 cytokine expressions in WAT of CHOP$^{+/+}$ mice (Figure 5A). In contrast, these HFD-induced downregulations of Th2 cytokines were attenuated in CHOP$^{-/-}$ mice (Figure 5A). Adipocytes per se are an important source of Th2 cytokines (Gordon, 2003). In particular, IL-13, the main Th2 cytokine in WAT, is reportedly produced mainly by adipocytes and modulates ATM polarization in a paracrine manner (Kang et al., 2008). Therefore, we

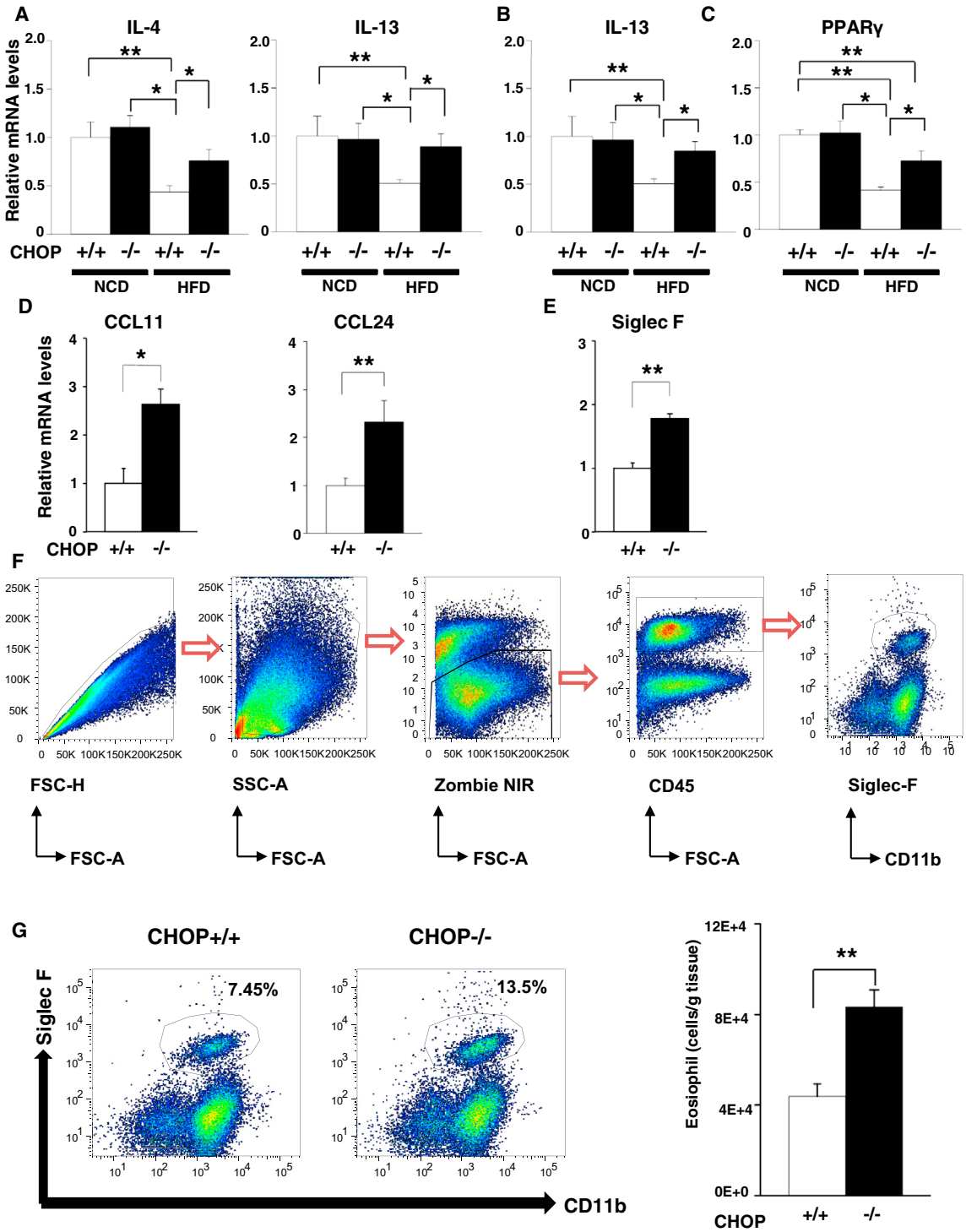

Figure 5. CHOP Deficiency Enhances Eosinophil Cell Recruitment in Adipose Tissue under HFD-Feeding Conditions

$CHOP^{+/+}$ (white bars) and $CHOP^{-/-}$ (black bars) mice were fed the HFD for 6 weeks.

(A) Relative amounts of mRNA for Th2 cytokines, IL-4 and IL-13, were measured in WAT of $CHOP^{+/+}$ (white bars) and $CHOP^{-/-}$ (black bars) mice fed NCD (n = 6–7 per group) and HFD (n = 11–12 per group).

(B and C) Relative amounts of mRNA for IL-13 (B) and PPARγ (C) were determined in the adipocyte fractions of WAT from $CHOP^{+/+}$ (white bars) and $CHOP^{-/-}$ (black bars) mice fed NCD and HFD (n = 6–9 per group).

(legend continued on next page)

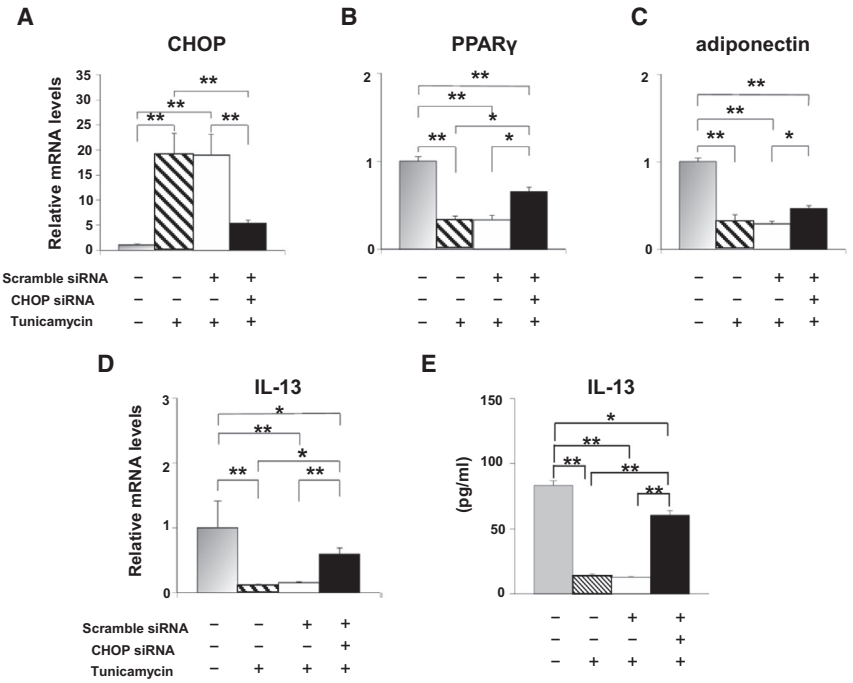

Figure 6. CHOP Upregulation in Adipocytes Is Involved in ER Stress-Induced Th2 Cytokine Downregulation in a Cell-Autonomous Manner

(A–D) Differentiated 3T3-L1 adipocytes were transfected with siRNAs for CHOP or scramble, followed by incubation with or without tunicamycin. Relative amounts of CHOP (A), PPARγ (B), adiponectin (C), and IL-13 (D) mRNA in 3T3-L1 adipocytes were determined (n = 5 per group).

(E) IL-13 concentrations in the cell culture media were measured (PBS and tunicamycin treated, n = 5 per group; control siRNA, n = 8; CHOP siRNA, n = 9). Data are presented as means ± SEM. Significance is indicated as follows: *p < 0.05, **p < 0.01 by one-way ANOVA.

next examined IL-13 expression in the adipocyte fractions obtained from WAT of CHOP$^{+/+}$ and CHOP$^{-/-}$ mice fed HFD. As observed in WAT, IL-13 expression was significantly higher in the adipocyte fractions obtained from HFD-fed CHOP$^{-/-}$ than in that from CHOP$^{+/+}$ mice (Figure 5B). IL-13 expression is reportedly upregulated according to adipocyte differentiation (Kang et al., 2008), which is reflected by PPARγ. In fact, although HFD feeding suppressed PPARγ expression in the adipocyte fractions of CHOP$^{+/+}$ mice (Figure 5C), the PPARγ downregulation was markedly inhibited by CHOP deficiency. Greater hypertrophy of adipocytes in CHOP$^{-/-}$ mice (Figure 2A) may be induced by sustaining PPARγ expression even after HFD. Collectively, these findings suggest that CHOP deficiency may sustain adipocyte function/differentiation, thereby maintaining Th2 cytokine secretion and ATM M2 polarization.

In addition, eosinophils were reported to be the major cell source of IL-4 production in WAT and to be decreased in WAT by HFD feeding (Wu et al., 2011). Chemokines, such as CCL11 (eotaxin-1) and CCL24 (eotaxin-2), are reportedly secreted by adipocytes and play important roles in recruiting eosinophils to WAT (Wu et al., 2011). Notably, both CCL11 and CCL24 were upregulated in WAT of CHOP$^{-/-}$ mice (Figure 5D). Furthermore, Siglec F, a surface marker of eosinophils (Figure 5E), was increased in the SV fractions of WAT. Furthermore, flow-cytometric analyses of the SV fractions of WAT (Figure 5F) revealed CD11b^{+}/Siglec F^{+} cells to be significantly increased in CHOP$^{-/-}$ mice (Figure 5G). These findings suggest that eosinophils residing in WAT also play a part in ATM M2 polarization of infiltrating macrophages, involving IL-4 production, in CHOP$^{-/-}$ mice. Taken together, these findings indicate that a Th2 cytokine-rich micro-environment is produced in the vicinity of ATMs by preserving adipocyte function and eosinophil recruitment, leading to ATM M2 polarization in CHOP$^{-/-}$ mice.

CHOP in Adipocytes Regulates IL-13 Expression in a Cell-Autonomous Manner

Next, to address the question of whether ER stress-induced CHOP upregulation in adipocytes is involved in Th2-cytokine downregulation and adipocyte dysfunction in a cell-autonomous manner, CHOP expression was knocked down in differentiated 3T3-L1 adipocytes, followed by analyzing gene expressions in vitro. Administration of tunicamycin, an ER stress inducer, markedly upregulated CHOP expression (Figure 6A), while downregulating the expressions of PPARγ (Figure 6B), adiponectin (Figure 6C), and IL-13 (Figure 6D). CHOP knockdown (Figure 6A) significantly suppressed ER stress-induced alterations in the expressions of these genes (Figures 6B–6D). Consistent with the mRNA level, IL-13 concentrations in the cell culture media were markedly decreased by tunicamycin treatment, but these decrements were suppressed by CHOP knockdown (Figure 6E). Thus, CHOP induction in response to ER stress in adipocytes is cell-autonomously involved in adipocyte dysfunction and Th2 cytokine downregulation.

(D and E) Relative amounts of mRNA for eotaxins (CCL11 and CCL24) in WAT of CHOP$^{+/+}$ (white bar, n = 13) and CHOP$^{-/-}$ (black bar, n = 15) mice (D) and an eosinophil cell marker, Siglec F (E), in the SV fractions obtained from WAT of CHOP$^{+/+}$ (white bar, n = 9) and CHOP$^{-/-}$ (black bar, n = 11) mice were determined by qRT-PCR.

(F) Representative FACS plot of SV fraction cells isolated from epididymal adipose tissue. The dot plots depict forward scatter (FSC) and side scatter (SSC) and the sequential gating strategy for analysis of eosinophils.

(G) The sequential gating for CD45^{+} and the eosinophil marker, Siglec F, positive cells in CHOP$^{+/+}$ (white bars) and CHOP$^{-/-}$ (black bars) mice (n = 5 per group). Data are presented as means ± SEM. Significance is indicated (*p < 0.05, **p < 0.01).

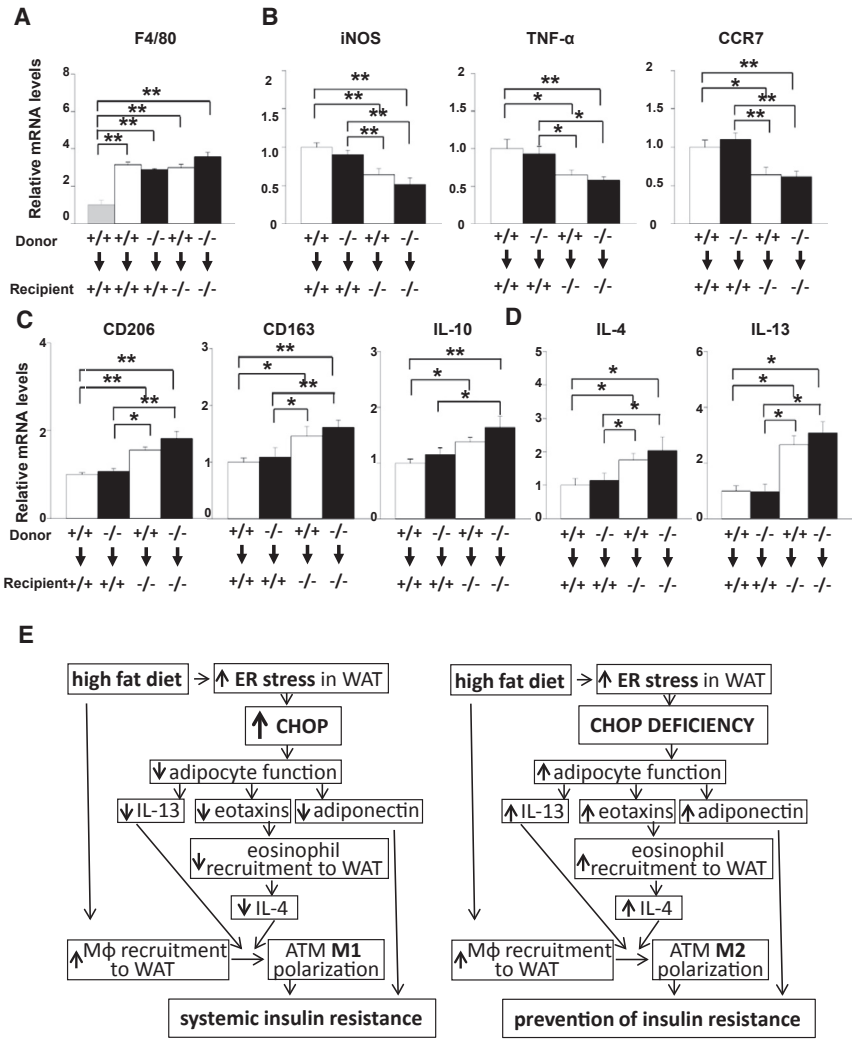

Figure 7. BMT Experiments Revealed the Importance of CHOP in Recipients in Determining ATM Polarization

Bone marrow cells from CHOP$^{+/+}$ and CHOP$^{-/-}$ mice were transplanted into lethally irradiated 6-week-old CHOP$^{+/+}$ and CHOP$^{-/-}$ mice (CHOP$^{+/+}$ to CHOP$^{+/+}$, n = 15; CHOP$^{-/-}$ to CHOP$^{+/+}$, n = 13; CHOP$^{+/+}$ to CHOP$^{-/-}$, n = 12; and CHOP$^{-/-}$ to CHOP$^{-/-}$, n = 8), followed by HFD feeding for 6 weeks.

(A) Relative amounts of mRNA for expressions of F4/80 in these mice were compared with those in CHOP$^{+/+}$ to CHOP$^{+/+}$ mice fed NCD for 6 weeks after BMT (gray bar, n = 8).

(B–D) Relative amounts of mRNA for expressions of M1 (B) and M2 (C) macrophage markers and Th2 cytokines, IL-4 and IL-13 (D), were determined in WAT by qRT-PCR. Data are presented as means ± SEM. *p < 0.05, **p < 0.01 by one-way ANOVA.

(E) Scheme of HFD-induced insulin resistance involving CHOP upregulation in WAT.

BMT Experiments Revealed the Importance of CHOP in Recipients in Determining ATM Polarization

Results obtained from our ex vivo and in vitro experiments suggest that CHOP upregulated in adipocytes, rather than that expressed in macrophages derived from bone marrow, altered micro-environmental conditions in the vicinity of infiltrating macrophages, thereby determining ATM polarization. Finally, to examine whether this holds true under in vivo conditions, we carried out BMT experiments. The BMT experiments, consisting of CHOP$^{+/+}$ to CHOP$^{+/+}$, CHOP$^{-/-}$ to CHOP$^{+/+}$, CHOP$^{+/+}$ to CHOP$^{-/-}$, and CHOP$^{-/-}$ to CHOP$^{-/-}$, were performed in 6-week-old mice. These mice were then fed the NCD or HFD for 6 weeks after BMT. As compared to NCD mice, expression of F4/80 was markedly increased in the WAT of CHOP$^{+/+}$ to CHOP$^{+/+}$ mice under HFD-feeding conditions (Figure 7A), confirming that the HFD loading actually increased macrophage infiltration into WAT under the experimental condition after BMT.

First, the F4/80 increment did not differ among the four BMT groups of mice fed HFD (Figure 7A), indicating similar degrees of WAT macrophage infiltration irrespective of donor and recipient genotypes. In contrast, expressions of the markers of M1 macrophages were significantly decreased in CHOP$^{+/+}$ to CHOP$^{-/-}$ and in CHOP$^{-/-}$ to CHOP$^{-/-}$, although CHOP deficiency in the donors did not significantly decrease these M1 marker expressions (Figure 7B). In addition, markers of M2 macrophages were also significantly increased when recipients were deficient in CHOP, including CHOP$^{+/+}$ to CHOP$^{-/-}$ and CHOP$^{-/-}$ to CHOP$^{-/-}$, but not when donors were CHOP deficient (Figure 7C). Furthermore, expressions of Th2 cytokines, both IL-4 and IL-13, in WAT were significantly increased when recipients were deficient in CHOP (Figure 7D). Again, donor CHOP deficiency did not significantly increase Th2 cytokine expressions (Figure 7D). These findings demonstrate that CHOP in recipients plays a major role in determining ATM polarization. These findings support the notion that adipose CHOP upregulation in response to HFD-induced ER stress suppresses micro-environmental conditions needed to inhibit M2 polarization of macrophages infiltrating WAT, resulting in chronic inflammation in WAT and insulin resistance at the whole-body level. The micro-environmental alterations in WAT may involve Th2 cytokine downregulation in adipocytes (Figure 7E).

DISCUSSION

The most interesting finding of this study is that CHOP deficiency induced ATM polarization to the M2 phenotype. It is well known that ATMs in lean animals show mostly the alternatively activated M2 phenotype, but that HFD feeding increases classically activated M1 macrophages, leading to the development of chronic inflammation in WAT and the progression of insulin resistance at the whole-body level (Fujisaka et al., 2009; Gordon, 2003;

Gordon and Taylor, 2005; Lumeng et al., 2007; Mantovani et al., 2004). In the present study, with normal chow feeding, expressions of a total macrophage marker as well as the polarity of ATMs were similar in $CHOP^{+/+}$ and $CHOP^{-/-}$ mice. HFD feeding upregulated CHOP expression in WAT, particularly in adipocytes of $CHOP^{+/+}$ mice, indicating that adipose ER stress was enhanced. Although HFD induced the ATM M1 phenotype to be predominant in $CHOP^{+/+}$ mice, CHOP deficiency resulted in ATMs remaining predominantly of the M2 phenotype despite similar amounts of macrophages infiltrating WAT. Furthermore, HFD-induced glucose intolerance as well as insulin resistance was prevented in $CHOP^{-/-}$ mice. These findings suggest that HFD-induced CHOP upregulation in WAT is involved in transition of infiltrating ATMs to the M1 phenotype and the resulting insulin resistance. Furthermore, BMT experiments clearly revealed recipient CHOP, rather than that expressed in bone marrow-derived cells, e.g., macrophages, to play a major role in ATM polarization. Although we do not rule out other mechanisms underlying the M1 transition during high-fat feeding, micro-environmental conditions in the vicinity of macrophages in WAT, rather than the presence or absence of CHOP in macrophages per se, appear to play important roles in determining ATM polarization.

There have been several reports regarding insulin resistance in $CHOP^{-/-}$ mice. Although female $CHOP^{-/-}$ mice reportedly gain weights with increased adiposity and hepatic steatosis (Ariyama et al., 2007; Maris et al., 2012), these mice maintain normal glucose tolerance associated with lower levels of pro-inflammatory cytokines (Maris et al., 2012). Thus, the observation that $CHOP^{-/-}$ mice exhibited a less insulin-resistant phenotype for the degree of obesity is essentially consistent with our findings. In contrast, Grant et al. (2014) reported that $CHOP^{-/-}$ mice fed HFD for a longer period became more insulin resistant with the development of hepatic steatosis. These conflicting results might give rise to apparent controversy. Even in this study, however, macrophages in adipose tissue were shown to be predominantly of the M2 phenotype. Therefore, the inconsistency may arise from differences in the degrees of hepatic insulin resistance due to the composition and/or the loading period of HFD as employed in these studies. Because CHOP deficiency also protects pancreatic β-cells from apoptosis, more severe hyperinsulinemia may lead to more fat accumulation in the liver with prolonged feeding of HFD. In the present study, pancreatic insulin contents as well as hepatic triglyceride contents were similar in $CHOP^{+/+}$ and $CHOP^{-/-}$ mice. Therefore, by selecting a shorter HFD loading period, we were able to clearly observe the role of adipose CHOP in determining ATM polarity and the resultant systemic insulin sensitivity with minimal effects from hepatocytes and pancreatic β-cells.

As for the factors that create micro-environmental conditions in WAT, Th2 cytokines, such as IL-4 and IL-13, which are reportedly produced and secreted by adipocytes, are well known to play a major role in maintaining ATM M2 macrophages (Gordon, 2003). In particular, IL-13 expression was reported to be dramatically induced during adipocyte differentiation (Kang et al., 2008). We showed that expressions of both IL-4 and IL-13 in WAT were greater in $CHOP^{-/-}$ than in $CHOP^{+/+}$ mice and that IL-13 expression was actually increased in the adipocyte fractions obtained from WAT of $CHOP^{-/-}$ mice. On the other hand, eosinophils are reported to be the major IL-4-secreting cells in WAT, thereby contributing to sustaining adipose M2 macrophages (Godfrey and Kronenberg, 2004; Kronenberg, 2005). Notably, HFD decreases eosinophil numbers and IL-4 levels in WAT (Godfrey and Kronenberg, 2004; Kronenberg, 2005; Wu et al., 2011). Eosinophil-recruiting chemokines, i.e., eotaxins, such as CCL11 and CCL24, are secreted by adipocytes (Badewa et al., 2002). In the present study, adipose expressions of CCL11 and CCL24 were higher in $CHOP^{-/-}$ than in $CHOP^{+/+}$ mice in the HFD-fed condition. Furthermore, RT-PCR and flow-cytometric analyses revealed eosinophils to be increased in the SV fractions of WAT of $CHOP^{-/-}$ mice, indicating eosinophil recruitment to WAT to be sustained by CHOP deficiency even after HFD loading. Collectively, these findings indicate that CHOP deficiency leads to ATM M2 polarization mediated by sustained Th2 cytokine production in adipocytes and eosinophils even after HFD loading. Taking these findings together with the observation that MCP-1 expression did not differ in adipose tissue of $CHOP^{+/+}$and $CHOP^{-/-}$ mice, ATM polarization might be affected after macrophage infiltration into WAT. Factors, such as Th2 cytokines and eotaxins, produced by adipocytes may be important for creating micro-environmental conditions and determining the fate of macrophages that have infiltrated WAT. Although whether CHOP directly or indirectly regulates Th2 cytokine expressions remains to be elucidated, our observations suggest that CHOP deficiency suppresses the M2-to-M1 transition of ATM by maintaining Th2 cytokine expressions in adipocytes.

In the present study, we showed that HFD upregulated not only CHOP but also other ER stress-related proteins, such as Bip, ATF4, and ATF6, in WAT, indicating increased ER stress in WAT under HFD-fed conditions. In $CHOP^{-/-}$ mice, PPARγ and adiponectin were significantly increased, despite apparent adipocyte hypertrophy, as compared with $CHOP^{+/+}$ mice in the HFD-fed condition. We further showed that, in cultured 3T3-L1 adipocytes, an ER stress inducer markedly upregulated CHOP expression and downregulated IL-13, PPARγ, and adiponectin expressions, but CHOP knockdown suppressed these downregulations. Furthermore, full adipocyte differentiation is reportedly accompanied by marked IL-13 upregulation (Kang et al., 2008). Taken together, these observations indicate that HFD-augmented ER stress in adipocytes may impair adipocyte function via CHOP upregulation, leading to reduced Th2 cytokine production. Decreased adiponectin production induced by impaired adipocyte function may concurrently contribute to the development of insulin resistance. CHOP was originally reported as a nuclear protein that dimerizes with C/EBP and inhibits its function (Ron and Habener, 1992). In addition, CHOP reportedly prevents adipocyte differentiation by directly interfering with C/EBPβ function (Adelmant et al., 1998). In the present study as well, CHOP knockdown prevented PPARγ and adiponectin downregulations by an ER stress inducer in 3T3-L1 adipocytes. Thus, in addition to UPR induction, CHOP plays an important role in modulating adipocyte function. The dual roles of CHOP may link ER stress responses with adipocyte dysfunction. Studies examining adipocyte-specific deficiency of CHOP, IL-13, C/EBPβ, and PPARγ may reveal the molecular mechanism underlying insulin resistance in more detail. Results from the BMT

experiments alone cannot rule out the contribution of cells other than adipocytes and hematopoietic cells in WAT, including vascular cells. However, the main source of IL-13 in WAT was reported to be adipocytes, and, in the present study, the in vitro results using cultured 3T3-L1 adipocytes with CHOP knockdown strongly suggest the importance of adipose CHOP in adipocyte dysfunction and ATM polarization under conditions of obesity.

In conclusion, CHOP deficiency inhibits chronic inflammation in WAT via ATM M2 polarization despite the infiltration of similar amounts of macrophages. Micro-environmental conditions, such as Th2 cytokine production by adipocytes, in WAT may play important roles in determining ATM polarization. CHOP in adipocytes is involved in the underlying mechanism (Figure 7E). Thus, adipose CHOP upregulation induced by HFD-promoted ER stress plays an important role in the development of insulin resistance and glucose intolerance during obesity development. This mechanism may constitute a potential therapeutic target for the metabolic syndrome.

EXPERIMENTAL PROCEDURES

Animals

Animal studies were approved by the institutional review board and conducted in accordance with the institutional guidelines for animal experiments at Tohoku University. CHOP-deficient mice (Oyadomari et al., 2001) were backcrossed for at least eight generations with C57BL/6J mice (Nippon CLEA). Wild-type ($CHOP^{+/+}$) and CHOP-deficient ($CHOP^{-/-}$) mice were kept on a 12-hr light/dark cycle with free access to food and sterile water. To achieve the HFD condition, mice were fed the HFD (32% sunflower oil, 33.1% casein, 17.6% sucrose, and 5.6% cellulose) for 6 weeks beginning at the age of 6 weeks.

Plasma Metabolic Parameters

Blood glucose, plasma insulin, adiponectin and leptin, serum total cholesterol, triglycerides, NEFA, MCP-1, and TNF-α concentrations were determined as described previously (Gao et al., 2007).

Pancreatic Insulin Contents

Pancreases were suspended in cold acid ethanol (1.5% HCl in 75% ethanol), minced with scissors, and left at 20°C for 48 hr, with sonication every 24 hr. Insulin contents in the acid ethanol supernatant were determined with an ELISA kit (Morinaga Institute of Biological Science) (Suzuki et al., 2011).

Glucose Tolerance Tests

Glucose tolerance tests (GTTs) were performed on fasted (10 hr) mice. Glucose (1 g/kg of body weight) was administered into the intraperitoneal space of the mice, and blood glucose was assayed immediately before and at 15, 30, 60, and 120 min post-administration.

Hyperinsulinemic-Euglycemic Clamp

Hyperinsulinemic-euglycemic clamp studies were performed as described previously (Gao et al., 2007), with slight modification. Chronically cannulated, conscious, and unrestrained mice were fasted for 6 hr before the study. Insulin (10 mU/kg/min) was infused throughout the clamp study. Blood glucose was monitored every 5 min via carotid arterial catheter samples. Glucose was infused at a variable rate to maintain blood glucose at 120 mg/dL. The GIRs were calculated as previously described (Jones et al., 2005). The GIR data obtained under 10 mU/kg/min of insulin clamp conditions reportedly reflect GLUT4-dependent tissues (i.e., muscle and adipose), because hepatic glucose output is totally suppressed by less than 2.5 mU/kg/min insulin (Ayala et al., 2006).

Oxygen Consumption

Oxygen consumption was measured with an O_2/CO_2 metabolism measuring system (model MK-5000RQ; Muromachikikai) as described previously (Yamada et al., 2006).

Locomotor Activity

Spontaneous locomotor activities of mice were analyzed with an infrared activity monitor (Supermex; Muromachikikai), as described previously (Hasegawa et al., 2012).

Isolation of Adipocyte and Stromal Vascular Fractions from Adipose Tissue

Epididymal adipose tissue was minced into fine pieces and digested with 1 mg/mL collagenase type 1, which was supplemented with 1% BSA (Sigma-Aldrich) solution at 37°C using a shaker for 1 hr and vortexed every 10 min. Then, the samples were filtrated through a mesh, 500 μL of EDTA were added, and then the samples were fractionated by brief centrifugation at 1,500 rpm for 5 min. The pellets and the floating cells were collected as the SV and adipocyte fractions, respectively.

qRT-PCR-Based Gene Expression

Total RNA was purified from WAT and the adipocyte and SV fractions from WAT using an ISOGEN kit (Wako Pure Chemical). Total RNA from monocytes/macrophages collected from the spleen, 3T3-L1 adipocytes, and blood, was purified using an RNeasy mini-kit (QIAGEN). The cDNA synthesized from total RNA was evaluated with a real-time PCR quantitative system as previously reported (Uno et al., 2006). The relative amount of mRNA was calculated with β-actin mRNA as the invariant control. The oligonucleotide primers are presented in Table S1.

Flow-Cytometric Analysis

Detailed procedures for flow-cytometric analysis are described in Supplemental Experimental Procedures. Briefly, cells in the SV fractions obtained from epididymal adipose tissues were treated with a Fixable Viability Kit, Zombie NIR-PBS (1:200; BioLegend), at room temperature for 15 min, followed by staining with antibodies to Brilliant Violet 421 anti-mouse F4/80 BM8 (1:100; BioLegend), FITC anti-mouse-CD45 (1:200; BioLegend), APC anti-mouse-CD11c (1:100; BioLegend), and PE rat anti-mouse SiglecF (1:50; BioLegend) for 30 min at 4°C in the dark. The samples were then fixed with a Cytofix/Cytoperm Plus Fixation/Permeabilization Kit (BD Biosciences) for 20 min at 4°C. In addition, the cells were stained with antibody to PE anti-mouse CD206 (MMR) (1:100; BioLegend). Data were acquired on a FACSCanto II flow cytometer (BD Biosciences) and analyzed with FlowJo software (Tree Star).

Cell Culture, Differentiation, and Transfection

Maintenance of 3T3-L1 and differentiation of 3T3-L1 cells were described previously (Gao et al., 2007). Mouse CHOP small interfering RNAs (siRNAs) and control siRNAs were designed in conjunction with Thermo Fisher Scientific. siRNAs and the transfection reagent DharmaFECT (Thermo Fisher Scientific) were added to the medium, followed by incubation for 24 hr at 37°C. Then, siRNA-transfected 3T3-L1 cells were incubated with 2 μg/mL tunicamycin for 12 hr. The concentrations of IL-13 in the cell culture media were measured 4 hr later, after switching to a different medium using Assay Kits (Abcam).

Ex Vivo Treatment of Macrophages

Detailed procedures for collection of macrophages are described in Supplemental Experimental Procedures. Isolated macrophages were incubated with 20 ng/mL recombinant murine IFN-γ (PeproTech) or 10 ng/mL recombinant murine IL-13 (PeproTech) for 24 hr.

Histological Analysis

WAT samples were removed and fixed with 10% formalin and embedded in paraffin. Tissue sections were stained with H&E. Total adipocyte areas were traced manually and analyzed. White adipocyte areas were measured in at least 100 cells per mouse in each group. The TUNEL assay kit (DeadEnd Fluorometric TUNEL system G3250; Promega) was used for quantification of apoptotic cells in WAT samples.

Immunohistochemical Detection of CD11c and CD206

The epididymal adipose tissues were excised, and then fixed overnight in 10% paraformaldehyde and embedded in paraffin. Samples were sectioned at 3 μm

and stained by the polymer method using a Histofine Mouse stain kit (Nichirei) for immunostaining with antibodies against CD11c (Thermo Fisher Scientific) at a dilution of 1:100 and CD206 (BD Pharmingen) at a dilution of 1:50. Immunoreactivity was visualized by incubation with a substrate solution containing 3,3′-diaminobenzidine tetrahydrochloride. Sections were stained with hematoxylin, dehydrated, and mounted with a coverslip.

Irradiation and Bone Marrow Transplantation

The $CHOP^{+/+}$ and $CHOP^{-/-}$ recipient mice underwent lethal irradiation (10 Gy) at 6 weeks of age and then received 4×10^6 freshly prepared sterile bone marrow cells obtained from $CHOP^{+/+}$ and $CHOP^{-/-}$ mice via tail vein injection (Gao et al., 2011). The mice were fed HFD (32% sunflower oil, 33.1% casein, 17.6% sucrose, and 5.6% cellulose) for 6 weeks after BMT. As a control for the BMT groups, a group of $CHOP^{+/+}$ to $CHOP^{+/+}$ mice were fed NCD for 6 weeks after BMT.

Statistical Analysis

All statistical analyses were performed with the Statistical Package for the Social Sciences, version 15.0 (SPSS Japan). All data were tested for normality employing the Kolmogorov-Smirnov test. When data were normally distributed, the statistical significance of differences was assessed using the unpaired t test and one-way ANOVA followed by Tukey post hoc analyses. When data were not normally distributed, the statistical significance of differences was judged based on p values using the Mann-Whitney U test.

SUPPLEMENTAL INFORMATION

Supplemental Information includes Supplemental Experimental Procedures, five figures, and one table and can be found with this article online at http://dx.doi.org/10.1016/j.celrep.2017.01.076.

AUTHOR CONTRIBUTIONS

T.S. and J.G. performed the biological experiments, analyzed the data, and prepared the figures and tables. J.G. and Y.I. conceived the projects and designed the experiments. J.G., Y.I., and H.K. wrote and edited the manuscript. K. Kondo, S.S., T.I., K.U., K. Kaneko, S.T., K.T., J.I., and T.Y. provided help and advice on the biological experiments. A.A. and N.I. provided help and advice on the FACS analyses. S.O. provided the mice and advice on the overall project. H.K. provided the overall project leadership.

ACKNOWLEDGMENTS

We thank T. Takasugi and J. Fushimi for technical assistance. We also appreciate the support of the Biomedical Research Core of Tohoku University Graduate School of Medicine. This work was supported by Grants-in-Aid for Scientific Research (25253067 to H.K. and 21591122 to Y.I.) and a Grant-in-Aid for Young Scientists (25860737 to J.G.) from the Japan Society for the Promotion of Science, and a Grant-in-Aid for Scientific Research on Innovative Areas (22126006 to H.K.) from the Ministry of Education, Culture, Sports, Science and Technology of Japan. This work was also supported by Creative Interdisciplinary Research Program funding from Tohoku University (to J.G.).

Received: August 28, 2015
Revised: December 14, 2016
Accepted: January 27, 2017
Published: February 21, 2017

REFERENCES

Adelmant, G., Gilbert, J.D., and Freytag, S.O. (1998). Human translocation liposarcoma-CCAAT/enhancer binding protein (C/EBP) homologous protein (TLS-CHOP) oncoprotein prevents adipocyte differentiation by directly interfering with C/EBPbeta function. J. Biol. Chem. *273*, 15574–15581.

Ariyama, Y., Shimizu, H., Satoh, T., Tsuchiya, T., Okada, S., Oyadomari, S., Mori, M., and Mori, M. (2007). Chop-deficient mice showed increased adiposity but no glucose intolerance. Obesity (Silver Spring) *15*, 1647–1656.

Ayala, J.E., Bracy, D.P., McGuinness, O.P., and Wasserman, D.H. (2006). Considerations in the design of hyperinsulinemic-euglycemic clamps in the conscious mouse. Diabetes *55*, 390–397.

Badewa, A.P., Hudson, C.E., and Heiman, A.S. (2002). Regulatory effects of eotaxin, eotaxin-2, and eotaxin-3 on eosinophil degranulation and superoxide anion generation. Exp. Biol. Med. (Maywood) *227*, 645–651.

Bi, M., Naczki, C., Koritzinsky, M., Fels, D., Blais, J., Hu, N., Harding, H., Novoa, I., Varia, M., Raleigh, J., et al. (2005). ER stress-regulated translation increases tolerance to extreme hypoxia and promotes tumor growth. EMBO J. *24*, 3470–3481.

Boutens, L., and Stienstra, R. (2016). Adipose tissue macrophages: going off track during obesity. Diabetologia *59*, 879–894.

Feuerer, M., Herrero, L., Cipolletta, D., Naaz, A., Wong, J., Nayer, A., Lee, J., Goldfine, A.B., Benoist, C., Shoelson, S., and Mathis, D. (2009). Lean, but not obese, fat is enriched for a unique population of regulatory T cells that affect metabolic parameters. Nat. Med. *15*, 930–939.

Fujisaka, S., Usui, I., Bukhari, A., Ikutani, M., Oya, T., Kanatani, Y., Tsuneyama, K., Nagai, Y., Takatsu, K., Urakaze, M., et al. (2009). Regulatory mechanisms for adipose tissue M1 and M2 macrophages in diet-induced obese mice. Diabetes *58*, 2574–2582.

Gao, J., Katagiri, H., Ishigaki, Y., Yamada, T., Ogihara, T., Imai, J., Uno, K., Hasegawa, Y., Kanzaki, M., Yamamoto, T.T., et al. (2007). Involvement of apolipoprotein E in excess fat accumulation and insulin resistance. Diabetes *56*, 24–33.

Gao, J., Ishigaki, Y., Yamada, T., Kondo, K., Yamaguchi, S., Imai, J., Uno, K., Hasegawa, Y., Sawada, S., Ishihara, H., et al. (2011). Involvement of endoplasmic stress protein C/EBP homologous protein in arteriosclerosis acceleration with augmented biological stress responses. Circulation *124*, 830–839.

Godfrey, D.I., and Kronenberg, M. (2004). Going both ways: immune regulation via CD1d-dependent NKT cells. J. Clin. Invest. *114*, 1379–1388.

Goerdt, S., Politz, O., Schledzewski, K., Birk, R., Gratchev, A., Guillot, P., Hakiy, N., Klemke, C.D., Dippel, E., Kodelja, V., et al. (1999). Alternative versus classical activation of macrophages. Pathobiology *67*, 222–226.

Gordon, S. (2003). Alternative activation of macrophages. Nat. Rev. Immunol. *3*, 23–35.

Gordon, S., and Taylor, P.R. (2005). Monocyte and macrophage heterogeneity. Nat. Rev. Immunol. *5*, 953–964.

Grant, R., Nguyen, K.Y., Ravussin, A., Albarado, D., Youm, Y.H., and Dixit, V.D. (2014). Inactivation of C/ebp homologous protein-driven immune-metabolic interactions exacerbate obesity and adipose tissue leukocytosis. J Biol Chem. *289*, 14045–14055.

Hasegawa, Y., Saito, T., Ogihara, T., Ishigaki, Y., Yamada, T., Imai, J., Uno, K., Gao, J., Kaneko, K., Shimosawa, T., et al. (2012). Blockade of the nuclear factor-κB pathway in the endothelium prevents insulin resistance and prolongs life spans. Circulation *125*, 1122–1133.

Ishihara, H., Takeda, S., Tamura, A., Takahashi, R., Yamaguchi, S., Takei, D., Yamada, T., Inoue, H., Soga, H., Katagiri, H., et al. (2004). Disruption of the WFS1 gene in mice causes progressive beta-cell loss and impaired stimulus-secretion coupling in insulin secretion. Hum. Mol. Genet. *13*, 1159–1170.

Jones, J.R., Barrick, C., Kim, K.A., Lindner, J., Blondeau, B., Fujimoto, Y., Shiota, M., Kesterson, R.A., Kahn, B.B., and Magnuson, M.A. (2005). Deletion of PPARgamma in adipose tissues of mice protects against high fat diet-induced obesity and insulin resistance. Proc. Natl. Acad. Sci. USA *102*, 6207–6212.

Kang, K., Reilly, S.M., Karabacak, V., Gangl, M.R., Fitzgerald, K., Hatano, B., and Lee, C.H. (2008). Adipocyte-derived Th2 cytokines and myeloid PPARdelta regulate macrophage polarization and insulin sensitivity. Cell Metab. *7*, 485–495.

Koh, Y.J., Kang, S., Lee, H.J., Choi, T.S., Lee, H.S., Cho, C.H., and Koh, G.Y. (2007). Bone marrow-derived circulating progenitor cells fail to transdifferentiate into adipocytes in adult adipose tissues in mice. J. Clin. Invest. *117*, 3684–3695.

Kronenberg, M. (2005). Toward an understanding of NKT cell biology: progress and paradoxes. Annu. Rev. Immunol. *23*, 877–900.

Lumeng, C.N., Bodzin, J.L., and Saltiel, A.R. (2007). Obesity induces a phenotypic switch in adipose tissue macrophage polarization. J. Clin. Invest. *117*, 175–184.

Mantovani, A., Sica, A., Sozzani, S., Allavena, P., Vecchi, A., and Locati, M. (2004). The chemokine system in diverse forms of macrophage activation and polarization. Trends Immunol. *25*, 677–686.

Maris, M., Overbergh, L., Gysemans, C., Waget, A., Cardozo, A.K., Verdrengh, E., Cunha, J.P., Gotoh, T., Cnop, M., Eizirik, D.L., et al. (2012). Deletion of C/EBP homologous protein (Chop) in C57Bl/6 mice dissociates obesity from insulin resistance. Diabetologia *55*, 1167–1178.

Nagel, S.A., Keuper, M., Zagotta, I., Enlund, E., Ruperez, A.I., Debatin, K.M., Wabitsch, M., and Fischer-Posovszky, P. (2014). Up-regulation of Bcl-2 during adipogenesis mediates apoptosis resistance in human adipocytes. Mol. Cell. Endocrinol. *382*, 368–376.

Nakatani, Y., Kaneto, H., Kawamori, D., Yoshiuchi, K., Hatazaki, M., Matsuoka, T.A., Ozawa, K., Ogawa, S., Hori, M., Yamasaki, Y., and Matsuhisa, M. (2005). Involvement of endoplasmic reticulum stress in insulin resistance and diabetes. J. Biol. Chem. *280*, 847–851.

Niwa, M., Sidrauski, C., Kaufman, R.J., and Walter, P. (1999). A role for presenilin-1 in nuclear accumulation of Ire1 fragments and induction of the mammalian unfolded protein response. Cell *99*, 691–702.

Oyadomari, S., and Mori, M. (2004). Roles of CHOP/GADD153 in endoplasmic reticulum stress. Cell Death Differ. *11*, 381–389.

Oyadomari, S., Takeda, K., Takiguchi, M., Gotoh, T., Matsumoto, M., Wada, I., Akira, S., Araki, E., and Mori, M. (2001). Nitric oxide-induced apoptosis in pancreatic beta cells is mediated by the endoplasmic reticulum stress pathway. Proc. Natl. Acad. Sci. USA *98*, 10845–10850.

Oyadomari, S., Koizumi, A., Takeda, K., Gotoh, T., Akira, S., Araki, E., and Mori, M. (2002). Targeted disruption of the Chop gene delays endoplasmic reticulum stress-mediated diabetes. J. Clin. Invest. *109*, 525–532.

Rapold, R.A., Wueest, S., Knoepfel, A., Schoenle, E.J., and Konrad, D. (2013). Fas activates lipolysis in a Ca^{2+}-CaMKII-dependent manner in 3T3-L1 adipocytes. J. Lipid Res. *54*, 63–70.

Ron, D., and Habener, J.F. (1992). CHOP, a novel developmentally regulated nuclear protein that dimerizes with transcription factors C/EBP and LAP and functions as a dominant-negative inhibitor of gene transcription. Genes Dev. *6*, 439–453.

Ron, D., and Walter, P. (2007). Signal integration in the endoplasmic reticulum unfolded protein response. Nat. Rev. Mol. Cell Biol. *8*, 519–529.

Sica, A., and Mantovani, A. (2012). Macrophage plasticity and polarization: in vivo veritas. J. Clin. Invest. *122*, 787–795.

Song, B., Scheuner, D., Ron, D., Pennathur, S., and Kaufman, R.J. (2008). Chop deletion reduces oxidative stress, improves beta cell function, and promotes cell survival in multiple mouse models of diabetes. J. Clin. Invest. *118*, 3378–3389.

Strissel, K.J., Stancheva, Z., Miyoshi, H., Perfield, J.W., 2nd, DeFuria, J., Jick, Z., Greenberg, A.S., and Obin, M.S. (2007). Adipocyte death, adipose tissue remodeling, and obesity complications. Diabetes *56*, 2910–2918.

Suzuki, T., Imai, J., Yamada, T., Ishigaki, Y., Kaneko, K., Uno, K., Hasegawa, Y., Ishihara, H., Oka, Y., and Katagiri, H. (2011). Interleukin-6 enhances glucose-stimulated insulin secretion from pancreatic beta-cells: potential involvement of the PLC-IP3-dependent pathway. Diabetes *60*, 537–547.

Uno, K., Katagiri, H., Yamada, T., Ishigaki, Y., Ogihara, T., Imai, J., Hasegawa, Y., Gao, J., Kaneko, K., Iwasaki, H., et al. (2006). Neuronal pathway from the liver modulates energy expenditure and systemic insulin sensitivity. Science *312*, 1656–1659.

Van Dyken, S.J., and Locksley, R.M. (2013). Interleukin-4- and interleukin-13-mediated alternatively activated macrophages: roles in homeostasis and disease. Annu. Rev. Immunol. *31*, 317–343.

Wang, J., Takeuchi, T., Tanaka, S., Kubo, S.K., Kayo, T., Lu, D., Takata, K., Koizumi, A., and Izumi, T. (1999). A mutation in the insulin 2 gene induces diabetes with severe pancreatic beta-cell dysfunction in the Mody mouse. J. Clin. Invest. *103*, 27–37.

Wellen, K.E., and Hotamisligil, G.S. (2003). Obesity-induced inflammatory changes in adipose tissue. J. Clin. Invest. *112*, 1785–1788.

Wu, D., Molofsky, A.B., Liang, H.E., Ricardo-Gonzalez, R.R., Jouihan, H.A., Bando, J.K., Chawla, A., and Locksley, R.M. (2011). Eosinophils sustain adipose alternatively activated macrophages associated with glucose homeostasis. Science *332*, 243–247.

Xu, H., Barnes, G.T., Yang, Q., Tan, G., Yang, D., Chou, C.J., Sole, J., Nichols, A., Ross, J.S., Tartaglia, L.A., and Chen, H. (2003). Chronic inflammation in fat plays a crucial role in the development of obesity-related insulin resistance. J. Clin. Invest. *112*, 1821–1830.

Yamada, T., Katagiri, H., Ishigaki, Y., Ogihara, T., Imai, J., Uno, K., Hasegawa, Y., Gao, J., Ishihara, H., Niijima, A., et al. (2006). Signals from intra-abdominal fat modulate insulin and leptin sensitivity through different mechanisms: neuronal involvement in food-intake regulation. Cell Metab. *3*, 223–229.